Synthesis and Binding Properties of Pyrimidine Oligodeoxynucleoside Analogs Containing Neutral Phosphodiester Replacements: The Formacetal and 3′-Thioformacetal Internucleoside Linkages

Robert J. Jones,* Kuei-Ying Lin, John F. Milligan, Shalini Wadwani, and Mark D. Matteucci*

Gilead Sciences, 346 Lakeside Drive, Foster City, California 94404

Received January 27, 1993

The replacement of the phosphodiester linkage with neutral, achiral, nuclease resistant entities is desirable for the development of oligodeoxynucleotide (ODN) analogs as therapeutic agents in either the antisense or antigene modes. Described herein is the use of the formacetal and 3′-thioformacetal connections as phosphodiester backbone analogs. Pyrimidine dimer blocks containing these moieties were synthesized and incorporated into ODNs in an alternating array with phosphodiester bonds, such that the ODNs had seven acetal and seven phosphodiester linkages. The binding properties of the resulting chimeric ODNs to single-stranded (ss) RNA and double-stranded (ds) DNA were then determined. ssRNA binding properties were determined by thermal denaturation (Tm) analysis, and the 3′-thioformacetal ODN/ssRNA duplex showed a 5.5 °C enhancement in Tm relative to the control phosphodiester ODN. The triple helix formation properties of the 3′-thioformacetal and formacetal ODNs were determined by footprint and restriction enzyme inhibition assays. The 3′-thioformacetal ODN binds to dsDNA with an affinity slightly less than the control ODN. The high affinity and specificity of an ODN containing the 3′-thioformacetal for the ssRNA target and dsDNA target suggest that this linkage is a promising analog for both antisense and triple helix therapeutic applications.

Oligodeoxynucleotide (ODN) analogs offer promise as therapeutic agents.[1] The development of technologies utilizing ODNs for the sequence-specific recognition of single-stranded RNA (ssRNA) and double-stranded DNA (dsDNA) have created the opportunity to modulate gene expression in vivo.[2] Two approaches for potential ODN therapy utilize antisense[3] or antigene[2] technologies.

Antisense ODNs anneal to complementary ssRNA by Watson–Crick hybridization and block RNA processing or translation.[3] Triple helix forming ODNs bind to dsDNA in a sequence specific manner and have the possibility of inhibiting transcription or replication at the chromosomal level.[2] In the most widely studied triplex binding motif, the third strand is composed of pyrimidine nucleotides and binds to homopurine sequences of DNA by Hoogsteen base pairing, in which thymine recognizes adenine–thymine base pairs and protonated cytosine recognizes guanine–cytosine base pairs. The pyrimidine third strand is oriented within the major groove of the duplex DNA parallel to the purine strand of the duplex. Triplex agents have been shown to block transcription factor binding[4a] and enzymatic cleavage of DNA in a site specific manner.[4b]

There are several obstacles that must be surmounted in order to improve the *in vivo* efficacy of ODN analogs. Unmodified ODNs are rapidly degraded by intracellular nucleases and unable to efficiently passively diffuse through cell membranes.[5] The major challenge of ODN analogs is to design backbone modifications which will increase the nuclease stability and cellular permeability while enhancing affinity. Several analogs of the phosphodiester backbone have been prepared which afford nuclease resistant derivatives. Phosphodiester analogs such as phosphorothioates,[6] phosphoramidates,[7] and methylphosphonates[8] confer nuclease stability to the corresponding ODNs but generate chirality at phosphorous. This asymmetry creates a complex mixture of 2^n diastereomers, where n is the number of modified linkages in the ODN, which ultimately lowers the affinity of the ODN for the target. A second class of backbone congeners replace the phosphodiester entity with neutral, achiral moieties. These include the carbonate,[9] carbamate,[10] morpholinocarbamate,[11] siloxane,[12] sulfide,[13] sulfone,[13b] sulfonate,[14] sulfonamate,[14] sulfamate,[15] and amine[16] linkages. These neutral modifications increase nuclease stability and

(1) (a) Riordan, M. L.; Martin, J. C. *Nature* **1991**, *350*, 442. (b) Matteucci, M. D.; Bischofberger, N. *Annu. Rep. Med. Chem.* **1991**, *26*, 287.

(2) Hélène, C.; Toulmé, J.-J. *Biochim. Biophys. Acta* **1990**, *1049*, 99.

(3) (a) Uhlmann, E.; Peyman, A. *Chem. Rev.* **1990**, *90*, 543. (b) *ODNs: Antisense Inhibitors of Gene Expression*; Cohen, J. S., Ed.; CRC Press: Boca Raton, FL, 1989.

(4) (a) Maher, L. J., III; Wold, B.; Dervan, P. B. *Science* **1989**, *245*, 725. (b) Maher, L. J., III; Dervan, P. B.; Wold, B. J. *Biochemistry* **1990**, *29*, 8820.

(5) Loke, S. L.; Stein, C. A.; Zhang, X. H.; Mori, K.; Nakanishi, M.; Subasinghe, C.; Cohen, J. S.; Neckers, L. M. *Proc. Natl. Acad. Sci. U.S.A.* **1989**, *86*, 3474.

(6) (a) Eckstein, F.; Gish, G. *TIBS (Trends in Biological Sciences)* **1989**, *14*, 97. (b) Eckstein, F. *Ann. Rev. Biochem.* **1985**, *54*, 367.

(7) Letsinger, R. L.; Singman, C. N.; Histand, G.; Salunkhe, M. *J. Am. Chem. Soc.* **1988**, *110*, 4470. Froehler, B.; Ng, P.; Matteucci, M. *Nucleic Acids Res.* **1988**, *16*, 4831. Froehler, B. C. *Tetrahedron Lett.* **1986**, *27*, 5575. Jäger, A.; Levy, M. J.; Hecht, S. M. *Biochemistry* **1988**, *27*, 7237.

(8) Miller, P. S.; Agris, C. H.; Aurelian, L.; Blake, K. R.; Murakami, A.; Reddy, M. P.; Spitz, S. A.; Ts'O, P. O. P. *Biochimie* **1985**, *67*, 769. Ts'O, P. O. P.; Miller, P. S.; Aurelian, L.; Murakami, A.; Agris, C.; Blake, K. R.; Lin, S.-B.; Lee, B. L.; Smith, C. C. *Ann. N.Y. Acad. Sci.* **1988**, *507*, 220.

(9) (a) Mertes, M. P.; Coats, E. A. *J. Med. Chem.* **1969**, *12*, 154. (b) Jones, D. S.; Tittensor, J. R. *J. Chem. Soc. D* **1969**, 1240. (c) Tittensor, J. R. *J. Chem. Soc. C* **1971**, 2656.

(10) (a) Gait, M. J.; Jones, A. S.; Walker, R. T. *J. Chem. Soc., Perkin Trans. 1* **1974**, 1684. (b) Coull, J. M.; Carlson, D. V.; Weith, H. L. *Tetrahedron Lett.* **1987**, *28*, 745. (c) Mungall, W. S.; Kaiser, J. K. *J. Org. Chem.* **1977**, *42*, 703. (d) Stirchak, E. P.; Summerton, J. E.; Weller, D. D. *J. Org. Chem.* **1987**, *52*, 4202.

(11) (a) Stirchak, E. P.; Summerton, J. E.; Weller, D. D. *Nucleic Acids Res.* **1989**, *17*, 6129. (b) Wang, H.; Weller, D. D. *Tetrahedron Lett.* **1991**, *32*, 7385.

(12) Ogilvie, K. K.; Cormier, J. F. *Tetrahedron Lett.* **1985**, *26*, 4159. Cormier, J. F.; Ogilvie, K. K. *Nucleic Acids Res.* **1988**, *16*, 4583.

0022-3263/93/1958-2983$04.00/0

potentially cellular permeability, but they also display lower affinity for the targets than the phosphodiester control. A third class replaces the sugar and phosphate with a polyamide backbone and has been termed peptide nucleic acids[17] and acyclic nucleic acids.[18]

A simple achiral solution to the problems of unmodified ODNs was to replace the phosphodiester with the formacetal linkage, which entailed substituting the phosphorous with a methylene group.[19,20] Replacement of the 5'-oxygen of this linkage with a sulfur has been reported, but the binding properties of the ODN containing this entity were poor.[19c] This work has now been extended by replacing the 3'-oxygen of the formacetal backbone with a sulfur. The 3'-thioformacetal phosphodiester mimic was incorporated into a pyrimidine ODN sequence in an alternating array with native phosphodiester bonds, such that the ODNs had seven 3'-thioformacetal and seven phosphodiester linkages. As measured by thermal denaturation (Tm) analysis, the resulting chimeric ODN demonstrated enhanced binding to ssRNA relative to the control ODN which only contained phosphodiester linkages. The triple helix formation properties of the 3'-thioformacetal and formacetal ODNs were determined by footprint and restriction enzyme inhibition assays. The 3'-thioformacetal ODN binds to dsDNA with an affinity slightly less than the control ODN. Herein is described the synthesis of the formacetal and 3'-thioformacetal linkages along with the ssRNA and dsDNA binding properties of the hybrid ODN sequences containing these moieties.

Results

The formacetal and 3'-thioformacetal moieties were incorporated into ODNs as dimer synthons. The target sequence required both thymidine–thymidine (T–T) and thymidine–cytidine (T–C) dimers. 5-Methyl-2'-deoxycytidine (C^M) was used in place of 2'-deoxycytidine since it has previously shown better binding properties in both duplex and triplex modes.[4a,21] Scheme I shows the synthesis of the formacetal linkage in both T–T and T–C^M dimers. 5'-DMT-3'-[(methylthio)methyl]thymidine (**1**)[19] was coupled with the 3'-(*tert*-butyldimethylsilyl) (TBS)-protected nucleosides, **2** or **3**, where the base is either thymidine (T) or 2'-deoxy-N^4-benzoyl-5-methylcytidine ($^{Bz}C^M$),[22] by treatment with bromine[23] in the presence of 2,6-diethylpyridine to afford the formacetal dimers **4** and **5** after removal of the silyl protecting groups with tetrabutylammonium fluoride (TBAF). These compounds were subsequently converted to the H-phosphonates **7** and **8** using 2-chloro-4*H*-1,3,2-benzodioxaphosphorin-4-one, **6**,[24] in the presence of pyridine followed by hydrolysis with aqueous triethylammonium bicarbonate (TEAB). Dimers **7** and **8** functioned as building blocks in solid-phase ODN synthesis using a H-phosphonate protocol.[25] Compounds **4** and **5** were also deblocked to provide the fully deprotected dimer blocks **21** and **22** as standards for nucleoside composition analysis.

Extension of the formacetal synthetic protocol to the 3'-thioformacetal analog gave poor yields of dimers, presumably due to the incompatibility of the thiol functionality with the oxidant and oxidation byproducts. Therefore, a different procedure was adopted which took advantage of the facile alkylation of a thiol moiety by a reactive chloromethyl ether electrophile. Scheme II shows the syntheses of the 3'-thioformacetal analogs as T–T and T–$^{Bz}C^M$ dimer blocks. The 3'-protected nucleosides **9** and **10** were chloromethylated using paraformaldehyde and dry hydrogen chloride[26] to deliver the chloromethyl ethers **11** and **12**. These derivatives were immediately coupled with 5'-DMT-3'-mercapto-3'-deoxythymidine, **13**,[27] in the presence of diisopropylethylamine (DIPEA) to yield the 3'-thioformacetal dimers **14** and **15** after removal of the ester protecting groups. Subsequent phosphitylation with **6** in pyridine followed by hydrolysis with aqueous triethylammonium bicarbonate (TEAB) afforded the H-phosphonates **16** and **17**. The dimer blocks **16** and **17** functioned as synthons for automated DNA synthesis. Compounds **14** and **15** were also deblocked to provide the fully deprotected dimer blocks **23** and **24** as standards for nucleoside composition analysis.

The T·T and T·$^{Bz}C^M$ formacetal and 3'-thioformacetal dimer blocks were incorporated into 15-mer ODNs by standard solid-phase DNA chemistry using a H-phosphonate protocol.[25] The sequences **18–20**, shown in Figure 1, were synthesized where the formacetal and 3'-thioformacetal linkages (T·T and T·C^M) were each alternated with standard phosphodiester linkages (p). The chimeric ODN **19** is a 15-mer which contains seven formacetal linkages alternating with seven phosphodiester linkages; analogously, ODN **20** is a 15-mer which contains seven 3'-thioformacetal linkages juxtaposed with seven phosphodiester linkages. ODN **18** serves as the control for binding studies and contains all phosphodiester linkages. The ODNs were deblocked and removed from the solid

(13) (a) Kawai, S. H.; Just, G. *Nucleosides Nucleotides* **1991**, *10*, 1485. (b) Huang, Z.; Schneider, K. C.; Benner, S. A. *J. Org. Chem.* **1991**, *56*, 3869. Schneider, K. C.; Benner, S. A. *Tetrahedron Lett.* **1990**, *31*, 335.

(14) Reynolds, R. C.; Crooks, P. A.; Maddry, J. A.; Akhtar, M. S.; Montgomery, J. A.; Secrist, J. A., III. *J. Org. Chem.* **1992**, *57*, 2983.

(15) Huie, E. M.; Kirshenbaum, M. R.; Trainor, G. *J. Org. Chem.* **1992**, *57*, 4569.

(16) (a) Vasseur, J.-J.; Debart, F.; Sanghvi, Y. S.; Cook, P. D. *J. Am. Chem. Soc.* **1992**, *114*, 4006. (b) Weis, A. L.; Hausheer, F. H.; Chaturvedula, P. V. C.; Delecki, D. J.; Cavanaugh, P. F., Jr.; Moskwa, P. S.; Oakes, F. T. *Compounds and Methods for Inhibiting Gene Expression*, International Patent WO 92/02534, 1992. (c) Matteucci, M.; Jones, R. J.; Munger, J. *Modified Internucleoside Linkages*, International Patent WO 92/05186, 1992.

(17) (a) Nielsen, P. E.; Egholm, M.; Berg, R. H.; Buchardt, O. *Science* **1991**, *254*, 1497. (b) Egholm, M.; Buchardt, O.; Nielsen, P. E.; Berg, R. H. *J. Am. Chem. Soc.* **1992**, *114*, 1895.

(18) Huang, S.-B.; Nelson, J. S.; Weller, D. D. *J. Org. Chem.* **1991**, *56*, 6007.

(19) (a) Matteucci, M. *Tetrahedron Lett.* **1990**, *31*, 2385. (b) Matteucci, M. *Nucleosides & Nucleotides* **1991**, *10*, 231. (c) Matteucci, M.; Lin, K.-Y.; Butcher, S.; Moulds, C. *J. Am. Chem. Soc.* **1991**, *113*, 7767.

(20) (a) Veeneman, G. H.; van der Marel, G. A.; van den Elst, H.; van Boom, J. H. *Recl. Trav. Chim. Pays-Bas* **1990**, *109*, 449. (b) Veeneman, G. H.; van der Marel, G. A.; van den Elst, H.; van Boom, J. H. *Tetrahedron* **1991**, *47*, 1547. (c) Quaedflieg, P. J. L. M.; van der Marel, G. A.; Kuyl-Yeheskiely, E.; van Boom, J. H. *Recl. Trav. Chim. Pays-Bas* **1991**, *110*, 435. (d) Quaedflieg, P. J. L. M.; Timmers, C. M.; Kal, V. E.; van der Marel, G. A.; Kuyl-Yeheskiely, E.; van Boom, J. H. *Tetrahedron Lett.* **1992**, *33*, 3081.

(21) (a) Lee, J. S.; Woodsworth, M. L.; Latimer, L. J. P.; Morgan, A. R. *Nucleic Acids Res.* **1984**, *12*, 6603. (b) Povsic, T. J.; Dervan, P. B. *J. Am. Chem. Soc.* **1989**, *111*, 3059. (c) Xodo, L. E.; Manzini, G.; Quadrifoglio, F.; van der Marel, G.; van Boom, J. H. *Nucleic Acids Res.* **1991**, *19*, 1505. (d) Xodo, L. E.; Manzini, G.; Quadrifoglio, F.; van der Marel, G.; van Boom, J. H. *Nucleic Acids Res.* **1991**, *19*, 5625.

(22) Divaker, K. L.; Reese, C. B. *J. Chem. Soc., Perkin Trans. 1* **1982**, 1171.

(23) Kihlberg, J. O.; Leigh, D. A.; Bundle, D. R. *J. Org. Chem.* **1990**, *55*, 2860.

(24) Marugg, J. E.; Tromp, M.; Kuyl-Yeheskiely, E.; van der Marel, G. A.; van Boom, J. H. *Tetrahedron Lett.* **1986**, *27*, 2661.

(25) Froehler, B. C.; Ng, P. G.; Matteucci, M. D. *Nucleic Acids Res.* **1986**, *14*, 5399.

(26) Hill, A. J.; Keach, D. T. *J. Am. Chem. Soc.* **1926**, *48*, 257.

(27) Cosstick, R.; Vyle, J. S. *J. Chem. Soc., Chem. Commun.* **1988**, 992.

Scheme I. Syntheses of Formacetal Backbone Linkages (T = Thymine; $^{Bz}C^{M}$ = N^4-Benzoyl-5-methylcytosine)

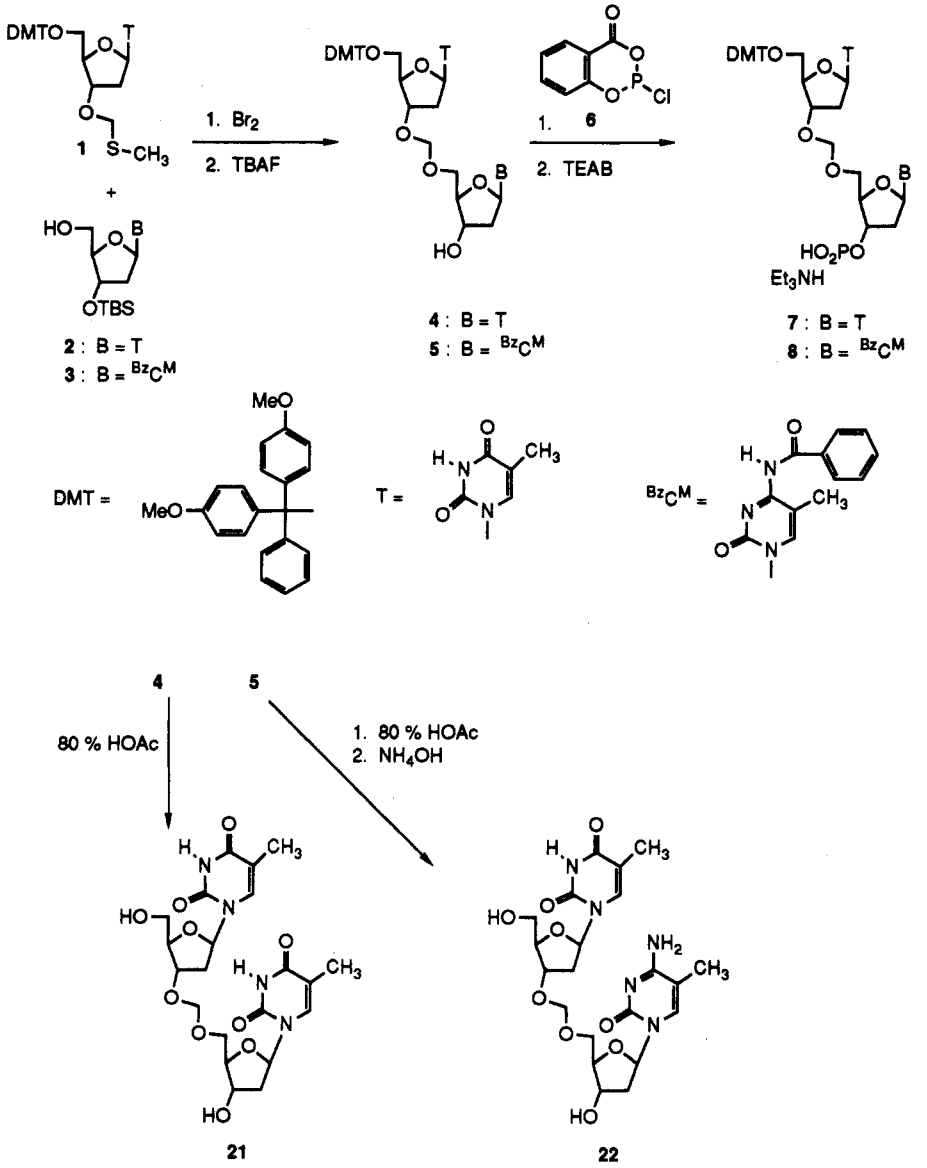

support by treatment with ammonium hydroxide, and purified by polyacrylamide gel electrophoresis (PAGE).

Each of the purified ODNs was homogeneous as assayed by PAGE and ion-exchange HPLC. The integrity of the formacetal and thioformacetal linkages after automated synthesis, deprotection, and purification was analyzed by nucleoside composition analysis.[28] The purified ODNs were simultaneously digested with nuclease P1 and alkaline phosphatase, and the resulting nucleoside mixture was analyzed by reversed-phase HPLC. ODN **19** displayed three peaks whose retention times corresponded to those of dimers **21**, **22**, and thymidine in a 2:5:1 ratio after correction for extinction coefficients. Similarly, ODN **20** gave three peaks whose retention times corresponded to those of dimers **23**, **24**, and thymidine in a 2:5:1 ratio after correction for extinction coefficients. Particular attention was paid to the fact that the 3′-thioformacetal linkage was not oxidized during the iodine oxidation used in the ODN synthesis protocol. These results demonstrated that the formacetal and 3′-thioformacetal backbone linkages can be utilized in automated ODN synthesis without complications.

The position of the formacetal and 3′-thioformacetal backbone linkages was confirmed by partial hydrolysis under acidic conditions.[19a] The ODNs were 3′-endlabeled using [α-^{32}P]cytidine triphosphate and terminal transferase, followed by RNase A treatment. The resulting purified, radiolabeled ODNs were partially cleaved with 90% formic acid at 90 °C, which selectively hydrolyzed the formacetal and 3′-thioformacetal linkages preferentially over the phosphodiester linkages.[19a] As shown in Figure 2, PAGE analysis of the formic acid cleavage products followed by autoradiography showed seven bands for acetal ODNs **19** and **20** corresponding to the seven analog linkages. The phosphodiester ODN control **18** showed no significant cleavage under these conditions.

The stability of the duplexes derived from ODNs **18**, **19**, and **20**, when hybridized to the complementary ssRNA **25**[29] and a sequence containing single base (G for A) mismatch **26**, was determined by thermal denaturation (Tm) analyses. These sequences are shown in Figure 1. The concentration of all ODNs was 2.8 μM, and the following buffer was used: 140 mM KCl; 5 mM Na_2HPO_4 (10 mM Na^+); 1 mM $MgCl_2$; and pH 7.2. These salt

(28) Eadie, J. S.; McBride, L. J.; Efcavitch, J. W.; Hoff, L. B.; Cathcart, R. *Anal. Biochem.* **1987**, *165*, 442.

(29) Lyttle, M. H.; Wright, P. B.; Sinha, N. D.; Bain, J. D.; Chamberlain, A. R. *J. Org. Chem.* **1991**, *56*, 4608.

5′ d(T•C^{M}pT•C^{M}pT•C^{M}pT•C^{M}pT•C^{M}pT•TpT•TpT)

18: • = phosphodiester

19: • = formacetal linkage

20: • = 3′-thioformacetal linkage

p = phosphodiester linkage

ssRNA sequences

25: 3′ AGAGAGAGAGAAAAA

26: 3′ AGAGGGAGAGAAAAA

Figure 1. ODN sequences: d denotes 2′-deoxyribonucleosides; C^{M} = 5-methyl-2′-deoxycytidine.

Scheme II. Syntheses of 3′-Thioformacetal Backbone Linkages (T = Thymine; $^{Bz}C^{M}$ = *N*^{4}-Benzoyl-5-methylcytosine)

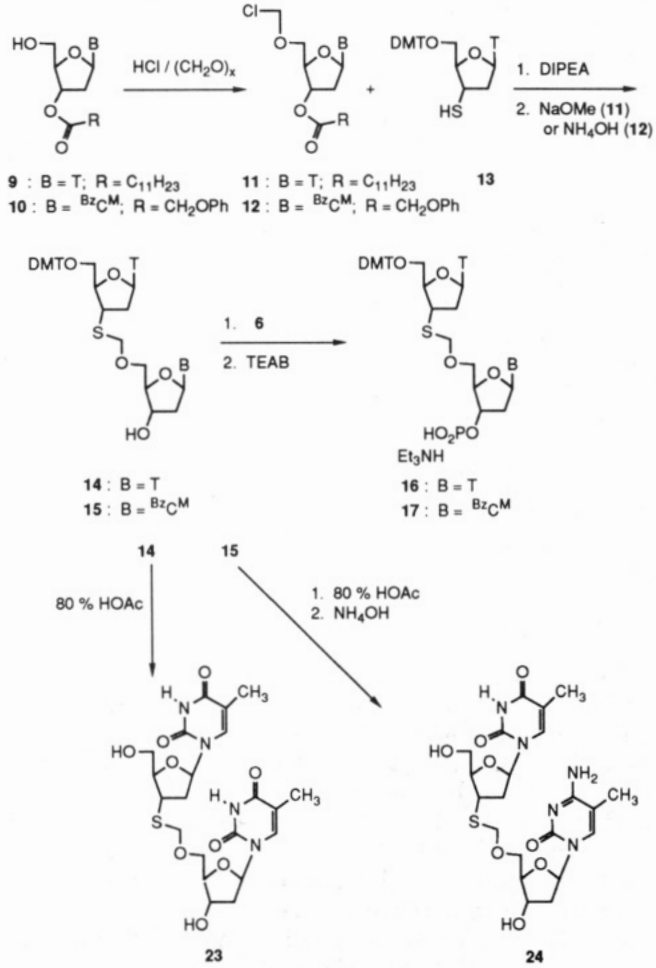

conditions were chosen to approximate the intracellular cationic environment.[30] The Tms were measured by both denaturation and renaturation modes. The data, as shown in Table I, show that the Tm of the formacetal ODN **19** is lower than the diester control **18** by 5.0 °C. The 3′-thioformacetal ODN **20**, however, displayed an increase in Tm of +5.5 °C relative to the control ODN **18**.

To test for specificity of hybridization, the Tms of the duplexes of **18**, **19**, and **20** were measured with the RNA ODN **26** which contains a one-base mismatch. Each ODN showed a −2.0 °C lower Tm than the duplexes of the exact

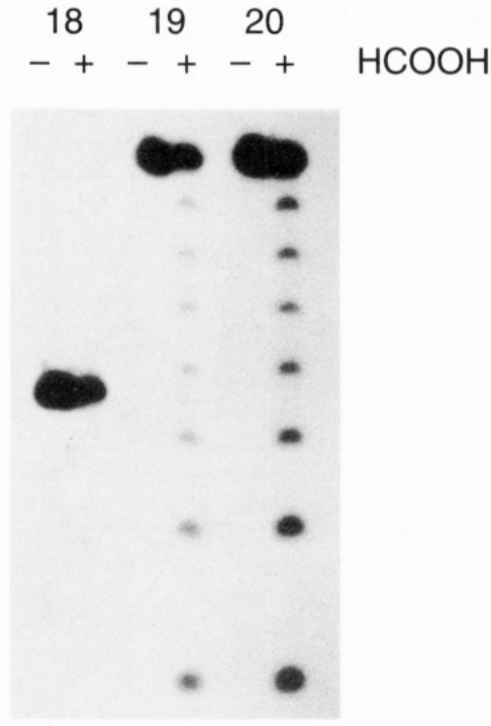

Figure 2. Autoradiogram of linkage mapping of ODNs **18**, **19**, and **20**. ODNs were incubated with (+) and without (−) 90% formic acid. Control diester ODN **18** and the 3′-thioformacetal ODN **20** were incubated for 30 min at 90 °C; formacetal ODN **19** was incubated for only 10 min at 90 °C to prevent overdigestion.

Table I. Tms of ODN:ssRNA Duplexes (±0.5 °C). TMS Were Measured in Both Denaturation (denat) and Renaturation (renat) Modes

ssRNA	25	25	26	26
ODN	denat	renat	denat	renat
18	62.5	62.0	60.5	60.0
19	57.5	56.5	55.0	55.0
20	68.0	67.0	66.0	65.5

complements. The G:T base pair mismatch is a wobble structure and is the most stable mismatch possible.[31] Therefore, the ODNs **19** and **20**, which contain the formacetal and 3′-thioformacetal linkages, show no decrease in specificity in this context from the control ODN as measured by the thermal stability of the complex.

The binding of ODNs **18**, **19**, and **20** to dsDNA by triple helix formation was determined by DNase I footprint analysis.[32] Again, the conditions were selected to approximate the intracellular cationic environment (20 mM MOPS, 140 mM KCl, 10 mM NaCl, 1 mM $MgCl_2$, 1 mM spermine, and pH 7.2).[30] The target sequence was incorporated into a restriction fragment to provide information on specificity as well as binding affinity. The restriction fragment, shown schematically in Figure 3, contains four cassettes which only differ in the base at the fifth position, which was varied from guanine to adenine, thymine, or cytosine in cassettes 1–4, respectively. The ODNs described above (Figure 1) target cassette 2 of this plasmid, while cassettes 1, 3, and 4 each contain a one-base mismatch. The autoradiogram derived from the DNase I footprint analysis, shown in Figure 4, shows that the control diester **18** completely protects cassette 2 of the

(30) Alberts, B. et al. *Molecular Biology of the Cell*; Garland: New York, 1989; p 301.

(31) Werntges, J.; Steger, G.; Riesner, D.; Fritz, H.-J. *Nucleic Acids Res.* **1986**, *14*, 3773.

(32) Brenowitz, M.; Senear, D. F.; Shea, M. A.; Ackers, G. K. *Proc. Natl. Acad. Sci. U.S.A.* **1986**, *83*, 8462.

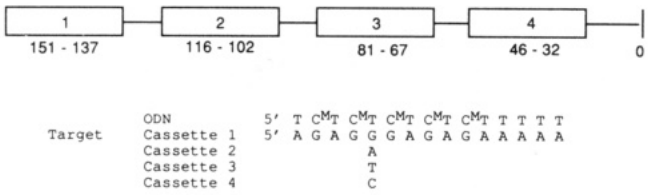

Figure 3. PvuII-SalI restriction fragment used in triple helix footprint assay. Four polypurine tracts were cloned into pUC19 to create p412. Each polypurine cassette is identical except for the base at the fifth position as shown. The specificity of triple helix formation is judged by the relative affinity of an ODN for its targeted cassette compared with the other cassettes. C^M = 5-methyl-2′-deoxycytidine.

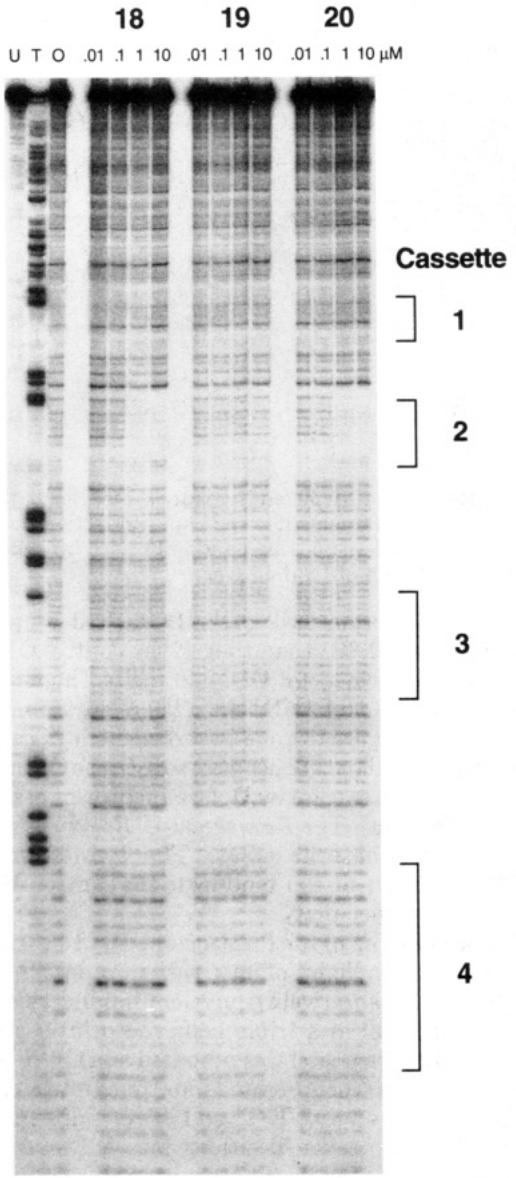

Figure 4. Autoradiogram of the DNase I triple helix footprint assay. ODNs **18**, **19**, and **20** were incubated at the indicated concentrations (μM) for 1 h at 37 °C. The U lane is the untreated PvuII-SalI restriction fragment. The T lane is a $KMnO_4$-treated sample to indicate the position of the thymidine residues. The O lane contains no ODN and is the DNase I digestion control. Each ODN is designed to bind to cassette 2. Protection from DNase I digestion is indicative of triple helix formation.

restriction fragment against DNase I digestion at 10 μM, and partial protection is seen at 1 μM. The formacetal ODN **19** shows no protection at all concentrations tested.

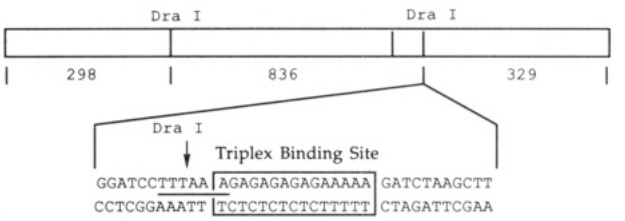

Figure 5. PCR DNA fragment used in the DraI restriction inhibition assay to determine K_ds. The size of each segment (in base pairs) is as shown. The DraI site which overlaps the triplex binding site is protected from cleavage upon binding by the ODN.

The 3′-thioformacetal ODN **20** displays similar protection to control ODN **18**, namely complete protection at 10 μM and partial protection at 1 μM. Cassettes 1, 3, and 4 showed no DNase I protection for ODNs **18** or **20** at any of the concentrations tested, thus demonstrating the single base specificity of the triple helix interaction for the 3′-thioformacetal analog and phosphodiester control.

The thermodynamic dissociation constants (K_ds) of the 3′-thioformacetal ODN **20** and the control **18** with their dsDNA target were determined using a modification of the restriction endonuclease protection assay of Maher et al.[4b] A restriction fragment, shown schematically in Figure 5, was constructed with a Dra I (TTTAAA) site which has a one-base overlap with the same 15 nucleotide polypurine sequence as cassette 2 in the footprint assay (Figure 3). The restriction fragment was radiolabeled by amplification using PCR and radiolabeled nucleotide triphosphates. This PCR fragment now contains two Dra I sites such that when both sites are cut with Dra I, restriction fragments of 446, 835, and 541 bp are created. When an ODN forms a triple helix at the polypurine target site, the Dra I cleavage is inhibited and restriction fragments of 1376 and 446 bp are generated. The generation of the 446 bp fragment resulting from the second Dra I site should not be affected by triple helix formation and thus serves as a control for the specificity of inhibition of Dra I cleavage. Samples of ODNs ranging in concentration from 0 to 10 000 nM were added to radiolabeled fragment (10 pM) and incubated at 37 °C for 1 h in the same buffer as the footprint assay except for the addition of 10 mM dithiothreitol (DTT). The reaction mixtures were treated with Dra I (40 units) for 2 min at 37 °C and quenched by addition of 15 mM EDTA in 10% aqueous glycerol. The radiolabeled fragments were separated by nondenaturing PAGE and visualized by autoradiography, shown in Figure 6a and b. The bands were cut out and quantitated by liquid scintillation counting. From Figure 7, the K_d was subsequently determined as the concentration of ODN at which 50% protection from endonuclease digestion was observed. The control ODN **18** binds with a K_d of 165 ± 15 nM and the 3′-thioformacetal ODN **20** binds with a K_d of 235 ± 5 nM.

Discussion

Replacement of the phosphodiester linkage of ODNs with neutral, achiral, nuclease resistant entities is desirable for the development of ODN analogs as therapeutic agents in either the antisense or antigene modes. The use of the formacetal and 3′-thioformacetal connections as phosphodiester backbone analogs in an alternating array with phosphodiesters is reported. Dimer blocks containing these moieties were readily synthesized in gram quantities.

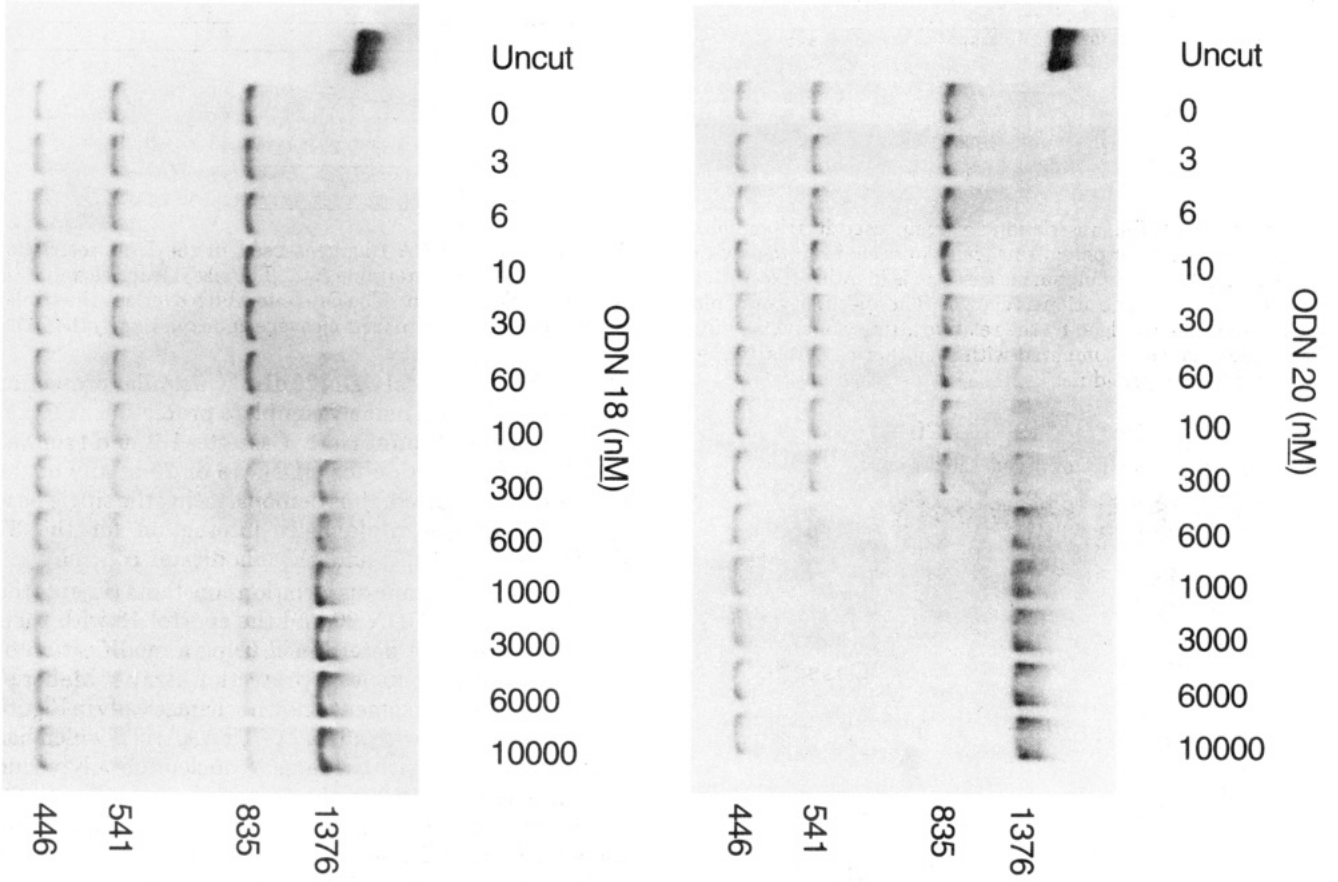

Figure 6. Autoradiograms of the DraI restriction assay. The radiolabeled PCR fragment (depicted in Figure 5) was incubated with increasing concentrations of ODN **18** (left) or ODN **20** (right). The uncleaved restriction fragment is 1822 bp. Protection from DraI cleavage is indicated by the presence of a 1376 bp band and the disappearance of the 835 and 541 bp bands. The 446 bp band is not affected by triple helix formation and serves as a control for the specificity of inhibition of DraI cleavage.

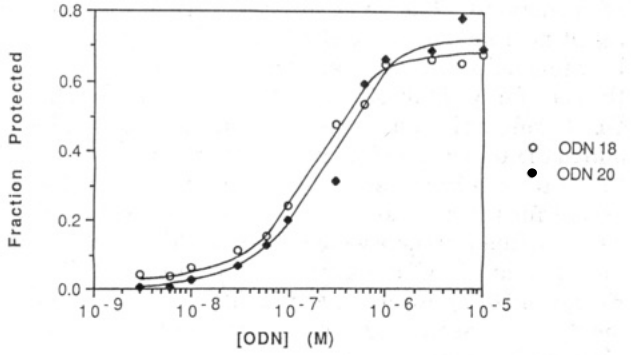

Figure 7. Analysis of the DraI restriction inhibition assay depicted in Figure 6. The 1376 bp bands were cut out of the gel, and the amount of radiolabeled DNA was determined by liquid scintillation counting. The data was fit to a theoretical curve, and the K_d was determined as the concentration of ODN which gives half of the total inhibition of DraI restriction.

The synthesis of the formacetal was similar to previous reports.[19] The construction of the 3′-thioformacetal utilized the nucleophilicity of a thiol with a chloromethyl ether, a potent alkylating moiety. The syntheses were performed with pyrimidine nucleosides thymidine and 5-methyl-2′-deoxycytidine.

The formacetal and 3′-thioformacetal dimer blocks were incorporated into ODNs in an alternating array with phosphodiester bonds such that the ODNs had seven acetal and seven phosphodiester linkages, and the resulting chimeric ODNs were purified and characterized. The binding affinities to ssRNA were determined by Tm analysis. The formacetal ODN **19** melted at a lower temperature (−5.0 °C) than that of the control ODN **18**, and the 3′-thioformacetal ODN **20** melted higher (+5.5 °C) than the control ODN **18**. There was no loss of specificity with regard to a one-base mismatch. The ODNs containing neutral backbones were subsequently analyzed for triple helix formation by DNase I footprint assay and K_d determination. The formacetal ODN **19** showed no binding in this footprint assay. The 3′-thioformacetal ODN **20** displayed similar binding to the control ODN **18** with no loss of specificity.

The poor binding of the formacetal ODN **19** to dsDNA was surprising in light of our earlier report[19c] which demonstrated qualitatively equivalent binding as a phosphodiester control in a triple helix footprint assay. In that work, the formacetal was prepared as a C^M–T dimer, and this dimer was incorporated four times into a 17-mer. In the present study, T–T and T–C^M dimers were incorporated into seven positions into a 15-mer. The higher percentage of analog linkages in an alternating array may be more stringent for helix formation and potentially amplify any inadequacies of the formacetal linkage. A second factor is the context difference, namely that the binding ability of analogs could be dependent on the nearest neighbors as has been seen previously for heterocycles.[33]

The difference between the binding characteristics of the phosphodiester, formacetal, and 3′-thioformacetal ODNs **18**, **19**, and **20**, respectively, can be rationalized by

(33) Griffin, L. C.; Dervan, P. B. *Science* **1989**, *245*, 967.

comparing the subtle differences between the length of the backbone linkage, the sugar pucker of the deoxyribose rings, and the torsion angles around the "anomeric" XCH_2O center. The length of the 3'-thioformacetal is ca. 0.5 Å longer than the formacetal[34] and therefore isometric with the native phosphodiester bond. The shorter formacetal bond may not allow the compound to achieve the optimum conformation for ssRNA duplex or dsDNA triplex binding. The sugar pucker of the deoxyribose and 3'-thiodideoxyribose could be different. The deoxyribose ring prefers the 2'-endo conformation,[35] and this sugar pucker will be affected by the substitution of the larger, less electronegative sulfur for oxygen. An ODN containing the T–T formacetal has been studied by NMR.[36] In a DNA–DNA duplex containing one T–T formacetal linkage, the sugar pucker was determined to be 2'-endo, and the structural perturbations due to the substitution of the formacetal moiety for the phosphodiester in B form duplex DNA were minimal.[36]

The difference between the binding characteristics of the 3'-thioformacetal and the 5'-thioformacetal, which was previously reported to display poor binding in the triplex mode, can be rationalized by steric considerations. Sulfur in the 5'-position could have negative steric interactions with either the ribosyl oxygen or the H6 of pyrimidine base relative to oxygen in that position. To gain a better understanding of the subtle differences between the phosphodiester, formacetal, and 3'- and 5'-thioformacetal linkages, a more detailed investigation of both the dimer blocks and the chimeric ODNs by high-field NMR[37] or crystallography[38] will be required.

The 3'-thioformacetal linkage was incorporated in an alternating array with phosphodiesters to afford a hybrid ODN. This compound displays a higher binding affinity against ssRNA than the diester control ODN. In triplex formation, it shows similar binding as the control ODN with no detectable loss of specificity. The replacement of the negatively charged phosphodiester linkage with 3'-thioformacetal should given the ODN greater stability to nucleases and, in principle, better cellular permeation characteristics. The high affinity and specificity for ss and ds target sequences, along with the promise of more favorable pharmacokinetic properties, demonstrate that the 3'-thioformacetal linkage is a promising phosphodiester analog for ODN agents, particularly directed against messenger RNA in therapeutic applications.

Experimental Section

^1H and ^{13}C NMR spectra were recorded at 300 and 75 MHz, respectively. High-resolution fast atom bombardment mass spectra analyses were performed by the Mass Spectrometry Laboratory at the University of California, Berkeley.

Automated Synthesis of all ODNs used H-phosphonate technology.[25] RNA was synthesized using the phosphoramidite procedure.[29] ODNs were deprotected using 7 M NaOH at 55 °C for 18 h. All ODNs were purified by PAGE. The appropriated bands were cut out and crushed. The purified ODN was extracted with 1 M ammonium acetate. The solvent volume was reduced by butanol extraction, and the ODNs were desalted using sephadex NAP column. ODN concentrations were determined from absorbance at 260 nm using extinction coefficients (M^{-1}, cm^{-1}) of 8700 (T) and 7400 (C^M).

Thymidine–Thymidine Formacetal (4). A mixture of 5'-*O*-DMT-3'-*O*-[(methylthio)methyl]thymidine (1) (0.9 g, 1.5 mmol), 3'-*O*-(*tert*-butyldimethylsilyl)thymidine (2) (0.8 g, 2.2 mmol), 2.6-diethylpyridine (1.0 g, 7.4 mmole), and molecular sieves (4 Å, 2 g) in dry benzene (60 mL) was stirred at room temperature for 1 h, followed by addition of bromine (1.0 M in benzene, 1.5 mmol). The resulting solution was then stirred at room temperature for 2 h and washed with saturated aqueous sodium bicarbonate solution. The organic layer was separated, dried (Na_2SO_4), and evaporated to dryness. The residual oil was dissolved in dry tetrahydrofuran (10 mL) and treated with tetrabutylammonium fluoride (1.0 M, 4.0 mmol) at room temperature for 30 min. The reaction was concentrated, dissolved in dichloromethane (DCM, 50 mL), washed with saturated aqueous sodium bicarbonate solution (2 × 50 mL), dried (Na_2SO_4), and evaporated to dryness. The residue was purified by flash column chromatography in triethylamine (TEA)/methanol (ME)/DCM (1:0:99–1:2.5:96.5) to afford 4 (0.84 g, 71%) as a colorless foam: ^1H NMR ($CDCl_3$) δ 7.62 (s, 1 H), 7.10–7.50 (m, 10 H), 6.83 (d, 4 H, J = 7.5 Hz), 6.20–6.40 (m, 2 H), 4.79 (q, 2 H, J = 12.3 Hz), 4.37 (m, 1 H), 4.28 (m, 1 H), 4.17 (m, 1 H), 4.06 (m, 1 H), 3.60–3.90 (m, 8 H), 3.52 (d, 1 H, J = 10.2 Hz), 3.34 (d, 1 H, J = 10.2 Hz), 2.05–2.80 (m, 4 H), 1.88 (s, 3 H), 1.49 (s, 3 H); ^{13}C NMR ($CDCl_3$) δ 164.11, 158.62, 150.92, 150.61, 144.18, 135.79, 135.43, 135.20, 135.14, 129.98, 128.93, 128.12, 127.96, 127.92, 127.09, 125.19, 113.20, 111,43, 110.83, 95.31, 93.32, 86.88, 85.17, 85.04, 84.36, 79.15, 71.52, 68.32, 63.48, 55.18, 40.10, 38.62, 21.36, 12.58, 11.80; HRMS (FAB) for $C_{42}H_{46}N_4O_{12}$ (MH^+) calcd 798.3112, found 798.3115.

H-Phosphonate 7. To a solution of 6 (1.0 M in DCM, 1.15 mL, 1.15 mmol), DCM (2 mL), and pyridine (1.9 g, 1.9 mmol) at 0 °C was added 4 (0.3 g, 0.376 mmol), in DCM (2 mL). The reaction mixture was stirred at room temperature for 2 h and then diluted with DCM (10 mL) and quenched with triethylammonium bicarbonate (TEAB, 1 M aqueous solution, 30 mL). The organic phase was dried (Na_2SO_4) and concentrated. Subsequent purification by flash chromatography in TEA/ME/DCM (0.5:2:97.5–0.5:10:89.5) delivered 7 (0.23 g, 64%): ^1H NMR ($CDCl_3$) δ 8.35 (s, 1 H), 8.27 (s, 1 H), 7.90 (s, $^1/_2$ H), 7.60 (s, 1 H), 7.10–7.50 (m, 10 H), 6.83 (d, 4 H, J = 7.5 Hz), 7.20–6.40 (m, 2 H), 5.85 (s, $^1/_2$ H), 4.65–4.95 (m, 3 H), 4.40 (m, 1 H), 4.25 (m, 1 H), 4.15 (m, 1 H), 3.60–3.90 (m, 8 H), 3.50 (d, 1 H, J = 10.2 Hz), 3.32 (d, 1 H, J = 10.2 Hz), 3.08 (q, 6 H, J = 15 Hz), 2.05–2.65 (m, 4 H), 1.85 (s, 3 H), 1.48 (s, 3 H), 1.35 (t, 9 H, J = 9.5 Hz).

Thymidine–5-Methyl-2'-deoxycytidine Formacetal (5). A mixture of 5'-*O*-DMT-3'-*O*-[(methylthio)methyl]thymidine (1) (1.0 g, 1.6 mmol), 2.6-diethylpyridine (0.45 g, 3.2 mmol), and molecular sieves (4 Å, 2 g) in dry benzene (12 mL) was stirred at room temperature for 1 h. Bromine (1 M in benzene, 1.6 mL) was added, followed by N^4-benzoyl-5-methyl-2'-deoxy-3'-*O*-(*tert*-butyldimethylsilyl)cytidine (2) (0.72 g, 1.6 mmol) in DCM (6 mL). The resulting mixture was stirred at room temperature for 3 h. The reaction mixture was filtered and concentrated. The residual oil was dissolved in DCM (25 mL), washed with saturated aqueous sodium bicarbonate solution, dried (Na_2SO_4), and concentrated. The crude product was purified by flash chromatography in TEA/ME/DCM (1:0:99–1:2.5:96.5). The isolated product was subsequently dissolved in tetrahydrofuran (5 mL) and treated with tetrabutylammonium fluoride (TBAF, 1.0 M, 5.0 mmol) at room temperature for 30 min. The reaction mixture was evaporated, redissolved in DCM (25 mL), and washed with saturated aqueous sodium bicarbonate solution. The organic phase was separated, dried (Na_2SO_4), and concentrated. The residue was purified by flash chromatography in TEA/ME/DCM (0.5:1:97.5–0.5:5:94.5), affording 5 (0.33 g, 23%): ^1H NMR ($CDCl_3$) δ 8.32 (d, 2 H, J = 7.5 Hz), 7.65 (s, 1 H), 7.54 (s, 1 H), 720–7.50 (m, 12 H), 6.84 (d, 4 H, J = 7.5 Hz), 6.35 (dd, 1 H, J_1 = 8.2 Hz, J_2 = 5.5 Hz), 6.28 (t, 1 H, J = 6.3 Hz), 4.8 (q, 2 H, J = 7.1 Hz), 4.40 (m, 1 H), 4.25 (m, 1 H), 4.19 (m, 1 H), 4.05 (m, 1 H), 3.70–3.86 (2 H), 3.78 (s, 6 H), 3.56 (dd, 1 H, J_1 = 10.4 Hz, J_2 = 2.4 Hz), 3.30 (dd, 1 H, J_1 = 10.4 Hz, J_2 = 2.3 Hz), 2.20–2.70 (m, 4 H), 2.07 (s,

(34) Gordon, A. J.; Ford, R. A. *The Chemist's Companion*; John Wiley & Sons: New York, 1972; p 108.
(35) Saenger, W. *Principles of Nucleic Acid Structure*; Springer-Verlag: New York, 1984.
(36) Gao, X.; Brown, F. K.; Jeffs, P.; Bischofberger, N.; Lin, K.-Y.; Pope, A. J.; Noble, S. A. *Biochemistry* **1992**, *31*, 6228.
(37) Witka, J. M.; Swaminathan, S.; Srinivasan, J.; Beveridge, D. L.; Bolton, P. H. *Science* **1992**, *255*, 597. Macaya, R. F.; Schultze, P.; Feigon, J. *J. Am. Chem. Soc.* **1992**, *114*, 781. Gao, X.; Jeffs, P. W. *J. Am. Chem. Soc.*, submitted.
(38) Arnott, S.; Selsing, E. *J. Mol. Biol.* **1974**, *88*, 509.

3 H), 1.60 (s, 3 H); ^{13}C NMR ($CDCl_3$) δ 163.62, 159.64, 158.74, 150.61, 147.83, 144.23, 137.08, 136.82, 135.44, 135.27, 135.10, 132.45, 130.09, 129.88, 128.09, 128.02, 127.22, 113.29, 111.61, 95.02, 87.01, 85.71, 85.27, 85.10, 84.45, 71.47, 68.04, 63.61, 55.30, 40.71, 38.52, 13.78, 11.87; HRMS (FAB) calcd for $C_{49}H_5N_5O_{12}Na$ (MNa^+) 924.3432, found 924.3441.

H-Phosphonate (8). A solution of **5** (100 mg, 0.11 mmol) in DCM (3 mL) and pyridine (48 mg, 0.6 mmol) was added to a 0 °C solution of **6** (1.0 M in DCM, 0.22 mL). The reaction was diluted with DCM (20 mL) and quenched with TEAB (1 M aqueous solution, 30 mL). The organic phase was isolated, dried (Na_2SO_4), and concentrated. The crude product was purified by flash chromatography in TEA/ME/DCM (0.5:2:97.5–0.5:10:89.5) to afford **8** (91 mg, 77%): ^{1}H NMR ($CDCl_3$) δ 13.25 (s, 1 H), 9.05 (s, 1 H), 8.32 (d, 2 H, J = 7.5 Hz), 7.92 (s, $^1/_2$ H), 7.60 (s, 1 H), 7.58 (s, 1 H), 7.20–7.58 (m, 12 H), 6.83 (d, 4 H, J = 7.5 Hz), 6.30–6.42 (m, 2 H), 5.86 (s, $^1/_2$ H), 4.79 (s, 2 H), 4.43 (m, 1 H), 4.28 (m, 1 H), 4.17 (m, 1 H), 3.91 (m, 1 H), 3.65–3.87 (8 H), 3.50 (d, 1 H, J = 10.5 Hz), 3.32 (d, 1 H, J = 10.5 Hz), 3.07 (q, 6 H, J = 15 Hz), 2.15–2.70 (m, 4 H), 2.10 (s, 3 H), 1.50 (s, 3 H), 1.35 (t, 9 H, J = 9.5 Hz).

3′-*O*-Dodecanoylthymidine (9). To a solution of 5′-*O*-DMT-thymidine (30.0 g, 55.0 mmol) in pyridine (275 mL) was added dodecanoyl chloride (25.4 mL, 110 mmol) dropwise, and the mixture was heated at 50 °C for 18 h. After being cooled to room temperature, the reaction was quenched with ME (25 mL) and concentrated in vacuo. The crude product was extracted with DCM (300 mL), washed with saturated aqueous sodium bicarbonate (300 mL), dried (Na_2SO_4), and concentrated. Toluene (2 × 200 mL) was added, and the solution was concentrated. The residual oil was dissolved in 10% ME in DCM (275 mL) and treated with *p*-toluenesulfonic acid (10.5 g, 55 mmol). After 0.5 h, the orange-red solution was quenched with saturated aqueous sodium bicarbonate (300 mL), and the organic layer was dried (Na_2SO_4) and concentrated. The crude product was dissolved in ethyl acetate (25 mL) and precipitated by addition of hexanes (250 mL) and cooling to −10 °C for 18 h. The mixture was filtered, and the precipitate was dried under high vacuum to afford **9** (11.3 g, 48%): ^{1}H NMR ($CDCl_3$) δ 9.67 (s, 1 H), 7.59 (s, 1 H), 6.29 (t, 1 H, J = 7.1 Hz), 5.36 (m, 1 H), 4.07 (d, 1 H, J = 2.2 Hz), 3.92 (bs, 2 H), 3.25 (bs, 1 H), 2.39 (m, 2 H), 2.34 (t, 2 H, J = 7.5 Hz), 1.90 (t, 3 H), 1.63 (t, 2 H, J = 7.1 Hz), 1.26 (bs, 16 H), 0.88 (t, 3 H, J = 6.5 Hz); ^{13}C NMR ($CDCl_3$) δ 173.58, 164.07, 150.59, 136.34, 111.24, 85.69, 85.20, 74.48, 62.38, 37.22, 34.10, 31.81, 29.50, 29.35, 29.22, 29.16, 29.03, 24.71, 22.59, 14.02, 12.47; HRMS (FAB) $C_{22}H_{37}N_2O_6$ (MH^+) calcd 425.2652, found 425.2659.

Thymidine–Thymidine Thioformacetal (14). Into a solution of 3′-*O*-dodecanoylthymidine **9** (2.12 g, 5.0 mmol), paraformaldehyde (225 mg, 7.5 mmol), and DCM (100 mL) at 0 °C was bubbled anhydrous hydrogen chloride for 10 min, and the solution was held at 4 °C for 48 h. The solution was thoroughly dried (Na_2SO_4), and the solvent was evaporated to afford the chloromethyl ether **11**. This chloromethyl ether was dissolved in DCM (25 mL) and added dropwise to a 0 °C solution of 3′-mercapto-5′-*O*-DMT-3′-deoxythymidine (**13**) (3.50 g, 6.25 mmol) and diisopropylethylamine (DIPEA, 2.18 g, 12.5 mmol) in DCM (100 mL). After being stirred for 3 h, the reaction mixture was quenched with saturated aqueous sodium bicarbonate (100 mL). The organic layer was separated, dried (Na_2SO_4), concentrated, and purified by flash chromatography in 2-propanol/DCM (1:99–5:95). The resulting product was treated with sodium methoxide (0.20 g, 3.64 mmol) in ME (20 mL) for 1 h. The reaction was quenched with acetic acid (0.21 mL, 3.64 mmol) and concentrated. The crude product was extracted with DCM, dried (Na_2SO_4), and purified by flash chromatography in ME/DCM (1:99–5:95) to deliver the product **14** (2.12 g, 52%): ^{1}H NMR ($CDCl_3$) δ 10.33 (bs, 1 H), 10.00 (bs, 1 H), 7.72 (s, 1 H), 7.42–7.19 (m, 8 H), 6.83 (d, 4 H, J = 8.4 Hz), 6.29 (t, 1 H, J = 6.5 Hz), 6.16 (t, 1 H, J = 5.0 Hz), 4.76 (bt, 2 H, J = 13 Hz), 4.39 (bs, 1 H), 4.19 (bs, 1 H), 4.13–4.03 (m, 2 H), 3.94–3.63 (m, 3 H), 3.77 (s, 6 H), 3.58 (bd, 1 H, J = 10.4 Hz), 3.56 (bd, 1 H, J = 8.6 Hz), 2.63 (m, 2 H), 2.38 (m, 1 H), 2.13 (m, 1 H), 1.88 (s, 3 H), 1.44 (s, 3 H); ^{13}C NMR ($CDCl_3$) δ 164.29, 158.60, 150.92, 150.66, 144.20, 135.82, 135.58, 135.24, 130.00, 128.02, 127.94, 127.10, 113.22, 110.93, 86.70, 85.41, 85.13, 84.96, 84.72, 73.73, 71.61, 68.55, 62.24, 55.20, 41.60, 41.08, 40.17, 12.62, 11.91; HRMS (FAB) for $C_{42}H_{46}N_4O_{11}S$ (M^+) calcd 814.2884, found 814.2874.

H-Phosphonate 16. To a solution of **6** (1.0 M in DCM, 1.15 mmol), DCM (5 mL), and pyridine (1.9 g, 1.9 mmol) at 0 °C was added **14** (0.27 g, 0.33 mmol) in DCM (2 mL). The reaction mixture was stirred at room temperature for 2 h, diluted with DCM (10 mL), and quenched with TEAB (1 M aqueous solution, 30 mL). The organic phase was dried (Na_2SO_4) and evaporated. Subsequent purification by flash chromatography in TEA/ME/DCM (0.5:2:97.5–0.5:10:89.5) delivered **16** (0.21 g, 65%): ^{1}H NMR ($CDCl_3$) δ 11.34 (s, 1 H), 11.31 (s, 1 H), 7.58 (s, $^1/_2$ H), 7.44–7.14 (m, 11 H), 6.86 (d, 4 H, J = 8.1 Hz), 6.12 (m, 2 H), 5.66 (s, $^1/_2$ H), 4.82 (m, 2 H), 4.56 (m, 1 H), 3.99 (m, 2 H), 3.72 (s, 6 H), 3.67 (dd, 1 H, J = 3.3, 10.5 Hz), 3.59 (dd, 1 H, J = 4.8, 10.8 Hz), 3.30 (m, 2 H), 3.07 (m, 6 H), 2.40 (m, 2 H), 2.13 (m, 2 H), 1.73 (s, 3 H), 1.48 (s, 3 H), 1.17 (t, 9 H, J = 7.3 Hz).

N^4-Benzoyl-5-methyl-2′-deoxy-3′-*O*-(phenoxyacetyl)cytidine (10). To a solution of N^4-benzoyl-5-methyl-5′-*O*-DMT-2′-deoxycytidine (10.0 g, 15.4 mmol) in pyridine (75 mL) at 0 °C was added phenoxyacetyl chloride (3.20 mL, 23.2 mmol) dropwise, and the mixture allowed to warm to ambient temperature over 18 h. The reaction was quenched with ME (25 mL) and concentrated in vacuo. The crude product was extracted with DCM (300 mL), washed with saturated aqueous sodium bicarbonate (300 mL), dried (Na_2SO_4), and concentrated. Toluene (2 × 100 mL) was added, and the solution was concentrated. The residual oil was dissolved in 10% ME in DCM (275 mL) and treated with *p*-toluenesulfonic acid (2.93 g, 15.4 mmol). After 0.5 h, the orange-red solution was quenched with saturated aqueous sodium bicarbonate (300 mL), and the organic layer was dried (Na_2SO_4) and concentrated. The crude product was dissolved in ethyl acetate (100 mL) and precipitated by addition of hexanes (100 mL) and cooling to −10 °C for 18 h. The solution was filtered, and the precipitate was dried under high vacuum to afford **10** (6.10 g, 82%): ^{1}H NMR ($CDCl_3$) δ 13.22 (bs, 1 H), 8.29 (d, 2 H, J = 7.0 Hz), 7.70 (s, 1 H), 7.52 (t, 1 H, J = 7.1 Hz), 7.43 (t, 2 H, J = 7.4 Hz), 7.31 (t, 2 H, J = 7.8 Hz), 7.01 (t, 1 H, J = 7.0 Hz), 6.92 (d, 2 H, J = 7.8 Hz), 6.22 (t, 1 H, J = 7.1 Hz), 5.50 (m, 1 H), 4.67 (s, 2 H), 4.14 (d, 1 H, J = 2.1 Hz), 3.93 (dq, 2 H, J = 2.3, 11.9 Hz), 3.00 (bs, 1 H), 2.46 (m, 2 H), 2.07 (s, 3 H); ^{13}C NMR ($CDCl_3$) δ 168.71, 159.47, 157.44, 148.05, 137.42, 136.85, 132.52, 129.83, 129.60, 128.09, 121.95, 114.53, 112.27, 86.39, 85.11, 75.78, 65.08, 62.32, 37.39, 13.62; HRMS (FAB) for $C_{25}H_{26}N_3O_7$ (MH^+) calcd 480.1771, found 480.1778.

Thymidine–5-Methyl-2′-deoxycytidine Thioformacetal (15). Into a solution of **10** (1.70 g, 3.55 mmol), paraformaldehyde (159 mg, 5.32 mmol), and DCM (75 mL) at 0 °C was bubbled anhydrous hydrogen chloride for 10 min, and the solution was held at 4 °C for 48 h. The solution was thoroughly dried (Na_2SO_4), and the volatiles were removed on the rotary evaporator to deliver the chloromethyl ether **12**. Compound **12** was subsequently dissolved in DCM (15 mL) and added dropwise to a solution of thiol **13** (1.43 g, 2.56 mmol) and DIPEA (0.826 G, 6.40 mmol) in DCM (75 mL) at 0 °C. After being stirred for 3 h, the reaction was quenched with aqueous saturated sodium bicarbonate (50 mL). The organic layer was separated, dried (Na_2SO_4), concentrated, and purified by flash chromatography in 2-propanol/DCM (1:99–5:95). The resulting dimer was treated with concd ammonium hydroxide (25 mL) in acetonitrile (25 mL) for 1 h. The volatiles were removed in vacuo. Ethanol (2 × 25 mL) was added, and the solution was again concentrated. Flash chromatography in ME/DCM (1:99–5:95) gave the product **15** (1.17 g, 50%): ^{1}H NMR ($CDCl_3$) δ 13.28 (bs, 1 H), 9.22 (s, 1 H), 8.31 (d, 2 H, J = 7.4 Hz), 7.72 (s, 1 H), 7.54–7.40 (m, 6 H), 7.31–7.24 (m, 7 H), 6.83 (d, 4 H, J = 8.2 Hz), 6.27 (t, 1 H, J = 6.42 Hz), 6.19 (t, 1 H, J = 5.6 Hz), 4.79 (dd, 2 H, J_1 = 12.1, J_2 = 15.6 Hz), 4.38 (m, 1 H), 4.06 (m, 2 H), 3.82 (m, 1 H), 3.79 (s, 6 H), 3.71 (q, 1 H, J = 6.0 Hz), 3.59 (dd, 1 H, J_1 = 1.9, J_2 = 10.8 Hz), 3.36 (dd, 1 H, J = 2.8, 10.8 Hz), 3.13 (d, 1 H, J = 3.4 Hz), 2.64 (t, 2 H, J = 6.5 Hz), 2.40 (m, 1 H), 2.18 (m, 1 H), 2.09 (s, 3 H), 1.50 (s, 3 H); HRMS (FAB) for $C_{49}H_{52}N_5O_{11}S$ (M^+) calcd 918.3384, found 918.3399.

H-Phosphonate 17. To a solution of **6** (1.0 M in DCM, 0.40 mL), DCM (5 mL), and pyridine (1.0 mL) at 0 °C was added **15** (0.18 g, 0.20 mmol) in DCM (2 mL). The reaction mixture was stirred at room temperature for 2 h, diluted with DCM (10 mL),

and quenched with TEAB (1 M aqueous solution, 30 mL). The organic phase was dried (Na_2SO_4) and concentrated. Subsequent purification by flash chromatography in TEA/ME/DCM (0.5:2:97.5–0.5:10:89.5) delivered 17 (0.14 g, 65.9%): ^{1}H NMR ($CDCl_3$) δ 13.28 (bs, 1 H), 12.40 (bs, 1 H), 9.02 (bs, 1 H), 8.31 (d, 2 H, J = 7.2 Hz), 7.94 (s, $^1/_2$ H), 7.64 (s, 1 H), 7.55 (s, 1 H), 7.51 (d, 1 H, J = 6.6 Hz), 7.46–7.39 (m, 5 H), 7.31–7.20 (m, 6 H), 6.83 (d, 4 H, J = 8.6 Hz), 6.34 (t, 1 H, J = 6.5 Hz), 6.18 (t, 1 H, J = 5.7 Hz), 5.88 (s, $^1/_2$ H), 4.81 (bs, 1 H), 4.73 (q, 2 H, J = 11.8, 19.6 Hz), 4.26 (d, 1 H, J = 2.7 Hz), 4.02 (d, 1 H, J = 7.5 Hz), 3.85 (m, 1 H), 3.77 (s, 6 H), 3.74–3.65 (m, 3 H), 3.59 (d, 1 H, J = 10.6 Hz), 3.36 (dd, 1 H, J = 2.3, 10.8 Hz), 3.07 (m, 6 H), 2.65–2.49 (m, 3 H), 3.16 (m, 1 H), 2.05 (s, 3 H), 1.44 (s, 3 H), 1.34 (t, 9 H, J = 7.3 Hz).

Determination of Base Composition. The base composition of each of the oligomers was confirmed by digestion of the oligomers and analysis by reversed-phase HPLC. The oligomers were converted to monomer and dimer nucleosides by incubation of 0.3 o.d. of oligomer with 10 units of P1 nuclease and 2 units of calf intestinal alkaline phosphatase (Boehringer–Mannheim) in 30 mM NaOAc, 1 mM $ZnSO_4$, and pH 5.2 overnight at 37 °C. The digested material was then injected directly onto a C18 column (Amicon, 100-Å pores) and the nucleosides separated by an acetonitrile gradient buffered with 50 mM potassium phosphate, pH 4.2. The retention times were then compared with monomer and dimer standards.

Formic Acid Treatment. ODNs **18**, **19**, and **20** were radiolabeled at their 3M termini by incubating with 10 pmol with 20 μCi of [α-^{32}P]cytidine triphosphate and terminal transferase in 100 mM cacodylate buffer (pH 7.0) and 1 mM $CoCl_2$ for 1 h at 37 °C. The mixture was then treated with RNase A (10 mg/mL) for 1 h at 37 °C. The radiolabeled oligonucleotides were subsequently purified by 20% denaturing PAGE using standard procedures. Approximately 10 000 cpm of ODN **19** was then treated with 80% formic acid at 94 °C for 10 min, and **18** and **20** were analogously treated for 30 min. The samples were lyophilized, resuspended in 100 μL of water, and lyophilized. Each sample was then suspended in 50% formamide with loading dyes and loaded onto a 20% (7 M urea) polyacrylamide gel. The samples were separated by electrophoresis and the resultant bands visualized by autoradiography.

Triple Helix Formation: Footprint Analysis. Duplex DNA target was labeled at the 3′ end SalI site with [α-^{32}P]-deoxycytosine triphosphate and Klenow fragment. Triple-strand hybridizations were performed at 37 °C for 1 h with 1 nM of radiolabeled DNA target (ca. 50 000 cpm) and increasing ODN concentrations (0.01, 0.1, 1, 10 μM) in the presence of 20 mM MOPS, 140 mM KCl, 10 mM NaCl, 1 mM $MgCl_2$, 1 mM spermine, and pH 7.2. The hybridization mixtures were treated with 1 unit of DNase I at 37 °C for 1 min and quenched by addition of 20 mM EDTA. The DNase I digestion products were analyzed by 5% denaturing PAGE and visualized by autoradiography.

Triplex Formation: K_d Determination. The thermodynamic dissociation constants (K_ds) of the 3′-thioformacetal ODN **20** and the control **18** were determined using a modification of the restriction endonuclease protection assay of Maher et al.[4b] A restriction fragment, which is schematically shown in Figure 5, was constructed with two Dra I (TTTAAA) sites such that one site has a one-base overlap with the triplex-binding site. The same 15 nucleotide polypurine target sequence as in the footprint assay was ligated into the Bam HI and Hind III sites in pUC19 to create pCTRI. pCRTI was digested with Bam HI and Hind III and the 1822 bp restriction fragment isolated. The restriction fragment was radiolabeled by amplification using PCR and radiolabeled nucleotide triphosphates. ODNs were added to 10 pM of radiolabeled plasmid and incubated at 37 °C for 1 h in the presence of 20 mM MOPS, 140 mM KCl, 10 mM NaCl, 1 mM $MgCl_2$, 1 mM spermine, 10 mM dithiothreitol (DTT) and pH 7.2. The reaction mixtures were treated with Dra I for 2 min and quenched by addition of 15 mM EDTA and 10% glycerol. The radiolabeled fragments were separated by PAGE and visualized by autoradiography. The appropriate bands were cut out and quantitated by scintillation counting. The K_d was subsequently determined at the concentration of ODN at which 50% protection from endonuclease digestion was observed.

RNA Tm Determination. 0.1 o.d. of ODN and 0.15 o.d. of target RNA were dissolved in 300 μL of buffer containing 140 mM KCl, 5 mM Na_2HPO_4, 1 mM $MgCl_2$, and pH 7.2 such that the final oligo concentration is 2.8 μM. The UV spectra were recorded at 260 nm from 25 to 90 °C (denaturation) and 90 to 25 °C (renaturation) at a ramp of 0.5 °C per min. The Tm was determined as the maximum of the first derivative of the absorbance vs temperature plot.

Acknowledgment. We thank Terry Terhorst for ODN syntheses, Matt Stephens for base composition analyses, and Brian Froehler for helpful discussions. This research was supported in part by grants from Defense Advanced Research Projects Agency (DARPA) and Small Business Innovation Research Program (SBIR).

Supplementary Material Available: Proton or carbon NMR spectra of compounds **4**, **7**, **5**, **8**, **9**, **14**, **16**, **10**, **15**, and **17** (10 pages). This material is contained in libraries on microfiche, immediately follows this article in the microfilm version of the journal, and can be ordered from the ACS; see any current masthead page for ordering information.